On the Mechanism of Stereospecific Polymerization—Development of a Universal Model to Demonstrate the Relationship between Metallocene Structure and Polymer Microstructure

Y. van der Leek, K. Angermund, M. Reffke, R. Kleinschmidt, R. Goretzki, and G. Fink*

Abstract: With the discovery of stereorigid bridged metallocenes, soluble catalysts became available for the stereospecific polymerization of α-olefins. A relatively simple mechanism was used to explain the stereospecificity, primarily in terms of the catalyst symmetry. In this paper we demonstrate that the simple rule of thumb that C_2-symmetric catalysts produce isotactic and C_s-symmetric catalysts syndiotactic polypropylene is too narrow. The introduction of one methyl group at the Cp ring in the [{*i*Pr(CpFlu)}ZrCl$_2$]/MAO system (Flu = fluorenyl, MAO = methylalumoxan) reduces the C_s symmetry to C_1, and the resulting catalyst produces hemiisotactic polypropylene. The analogous catalyst with a bulkier *tert*-butyl group at the Cp ring gives isotactic polypropylene. When the C_2 symmetry of [{Me$_2$Si(Ind)$_2$}ZrCl$_2$] (Ind = indenyl) is reduced to C_1, a metallocene can be obtained that produces atactic polypropylene. We have broken away from the symmetry-based model and developed a universal model, which accurately describes the experimental microstructures of the polymers by considering the four lowest-energy conformers of the metallocene species coordinating to prochiral propene (R_{re}, S_{re}, S_{si}, and R_{si}) and the positional changes that the polymer chain undergoes during insertion. The relative energy levels of the four diastereomers can be determined by molecular modeling calculations; these energy gradations, in particular the size of the energy gaps, are decisive in determining the stereospecificity. Also, the model permits the stereoerrors to be classified and explained. Through this model the stereosequence of a polymer chain can be calculated and predicted.

Keywords
asymmetric catalysis · metallocenes · polymerizations · molecular modeling · reaction mechanisms

Introduction

Soluble stereospecific catalysts for the polymerization of α-olefins became available for the first time as a result of work by Brintzinger[1] and Ewen.[2] With these defined stereorigid metallocenes it was possible to study the mechanism of stereospecific polymerization in more detail. An initial relatively simple mechanism explained the stereospecificity solely as a function of the catalyst symmetry. The C_2-symmetric [{Me$_2$Si(Ind)$_2$}ZrCl$_2$] and the C_s-symmetric [{*i*Pr(CpFlu)}ZrCl$_2$] catalysts each only have one favorable and one unfavorable coordination of the prochiral faces of the propene at the zirconium atom. Owing to steric congestion, the methyl group of the propene is normally directed away from the catalyst center, and a regioselective 1,2-insertion is then observed. Occasionally, the propene is coordinated the other way around causing 2,1-misinsertions (m-2,1 or r-2,1). The steric demand of the ligand determines the preferred orientation of the propene, which causes two diastereomeric complexes to form with different energy content. In the case of catalyst [{Me$_2$Si(Ind)$_2$}ZrCl$_2$], the same prochiral face of the propene is always favored during the polymerization, whereas the two prochiral faces of the propene are alternately favored in the case of catalyst [{*i*Pr(CpFlu)}ZrCl$_2$]. Thus, repeated coordination and insertion of propene produce isotactic polypropylene in the case of the [{Me$_2$Si(Ind)$_2$}ZrCl$_2$] catalyst and syndiotactic polypropylene in the case of the [{*i*Pr(CpFlu)}ZrCl$_2$] catalyst (lines 1 and 2 in Figure 1).

A multitude of catalysts have now been developed for the stereospecific production of a range of different polypropylenes.[3–9] It is now clear that the simple rule of thumb that C_2-symmetric catalysts produce isotactic and C_s-symmetric catalysts syndiotactic polypropylene is too narrow a definition of the requirements necessary for the stereospecific generation of polymers. Through the introduction of one methyl group at the Cp ring in the [{*i*Pr(CpFlu)}ZrCl$_2$]/MAO system, the C_s symmetry is lost. Now, this catalyst no longer produces a syndiotactic, but a hemiisotactic polypropylene, in which, alternately, the methyl groups are isotactically and statistically arranged (line 3 in Figure 1). On introduction of the bulkier *tert*-butyl group at the Cp ring (instead of the methyl group), the C_s symmetry is, of course, again destroyed. Perhaps surprising at first, an isotactic polypropylene is now formed (line 4 in Figure 1). Through

---

[*] G. Fink, Y. van der Leek, K. Angermund, M. Reffke, R. Kleinschmidt, R. Goretzki
Max-Planck-Institut für Kohlenforschung
Kaiser-Wilhelm-Platz 1, D-45470 Mülheim an der Ruhr (Germany)
Fax: Int. code +(208)306-2980

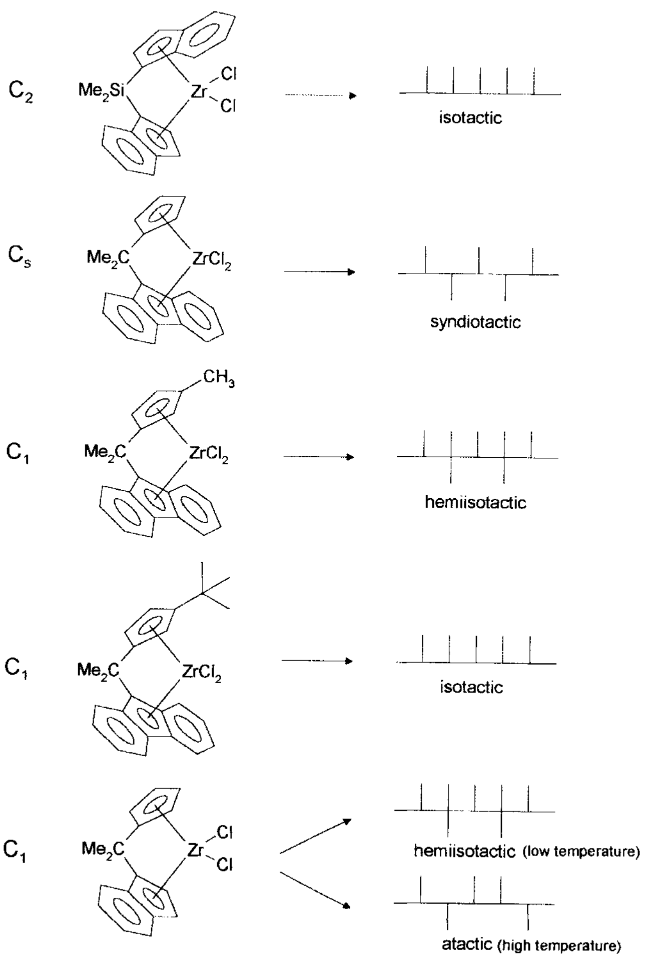

Figure 1. Structure and stereospecificity of metallocenes.

an appropriate symmetry reduction in C_2-symmetric [{Me$_2$Si-(Ind)$_2$}ZrCl$_2$] it is expected that a metallocene such as [{*i*Pr(CpInd)}ZrCl$_2$] (line 5 in Figure 1) should be produced that would give hemiisotactic polypropylene. Again, the result is surprising: hemiisotactic sequences are best formed at low temperatures, whereas completely atactic polypropylene is formed at room temperature and above.

Breaking away from the symmetry considerations, we have developed a more universal model, which accurately describes the experimental microstructures of the polymer by means of four lowest-energy conformers of the metallocene species coordinating prochiral propene (R_{re}, S_{re}, S_{si}, and R_{si}) and the positional changes that the polymer chain undergoes during insertion. The relative energy levels of the four diastereomers can be determined by molecular modeling calculations; these energy differences are decisive in determining the microstructures of the resulting polymers.

Our conformational calculations are based on primary work by Guerra and Corradini.[10–12] Their calculations, for instance, on [{*i*Pr(CpFlu)}Zr(isobutyl)(propene)] species and [{*i*Pr(3-Me-CpFlu)}Zr(isobutyl)(propene)] species, led to the following results: 1) Contrary to prior qualitative proposals, the ligand in the metallocene cation has no noteworthy interaction with the π-coordinated propene. 2) There is a strong interaction between the ligand and the growing polymer chain, which forces the latter to choose between two possible positions. In each case, the lowest-energy position is determined by the chirality of the catalyst. The interaction between the growing polymer chain and the methyl group of the propene causes the energy difference between *re* and *si* coordination; the methyl group of propene is always *trans* to the growing polymer chain. With an isospecific C_2-symmetric catalyst, the complexes have the same chirality after each insertion, which means that the propene is coordinated repeatedly in a *re* or *si* orientation. With a C_s-symmetric catalyst, it is important to note that the catalyst's two possible coordination positions are enantiomeric. The chirality of the complex changes after each insertion. Therefore, the propene is coordinated alternately in a *re* and *si* orientation.

Results and Discussion

Based on molecular modeling calculations by M. Nolte,[13, 16] results for the system [{*i*Pr(CpInd)}ZrCl$_2$][14] (bottom line, Figure 1) have already been obtained which were in good agreement with experimental data. Further detailed calculations have now been performed to explain the mechanism of the stereospecific polymerization with substituted [{*i*Pr(CpFlu)}-ZrCl$_2$] compounds.

A model to explain the tacticity change of the substituted [{*i*Pr(CpFlu)}ZrCl$_2$] catalyst was developed with the aid of force-field calculations using the program SYBYL[15] running on Silicon Graphics workstations. The valence force field applied appears as an extended TAFF force field[15] with special parameters for the zirconium environment.[13, 16] These valence force-field calculations relate to the geometric optimization of potential intermediate stages of the polymerization of propene with metallocenes. It is assumed that the polymerization takes place via a four-membered transition state with a cation as "active species". The calculated complexes represent potential intermediates, which can be thought of as lying shortly before the transition state of the polymerization process. The conformation of the intermediate state is decisive for the stereospecific insertion of the propene molecule. The influence of MAO, solvents, etc. on the stereospecificity is assumed to be constant for all compounds in these calculations. In order to present a clear account of the results to follow, we describe further details of the calculations in the Appendix.

We first consider the methylated cationic species (R = Me) coordinating a propene molecule. The molecular modeling calculations include two insertion steps for each catalyst (initially the alkyl chain is methyl, and then *i*Bu and (*R*)- or (*S*)-2,4-dimethylpentyl after the first and second insertions, respectively).

It should be emphasized that the energy values, obtained for each geometrically optimized catalyst, alone have no physical meaning, since the observed catalysts differ from one another in the number of atoms, bonds, and angles. Since the coordinated alkyl chains have also been varied, the energy values can only be compared within a given system (i.e., one catalyst with only one distinct alkyl chain).

According to Corradini,[11] a change in chirality takes place at the Zr during an insertion step (transfer from (*R*) to (*S*) and vice versa). An m diad is formed when propene is inserted twice in the *re* coordination mode. An r diad is formed through successive *re* and *si* coordination.

[{*i*Pr(CpFlu)}Zr(alkyl)(propene)]: During the polymerization of propene, the [{*i*Pr(CpFlu)}ZrCl$_2$] catalyst can react to form four possible diastereomeric intermediates (two pairs of enantiomers, Figures 2 and 3).

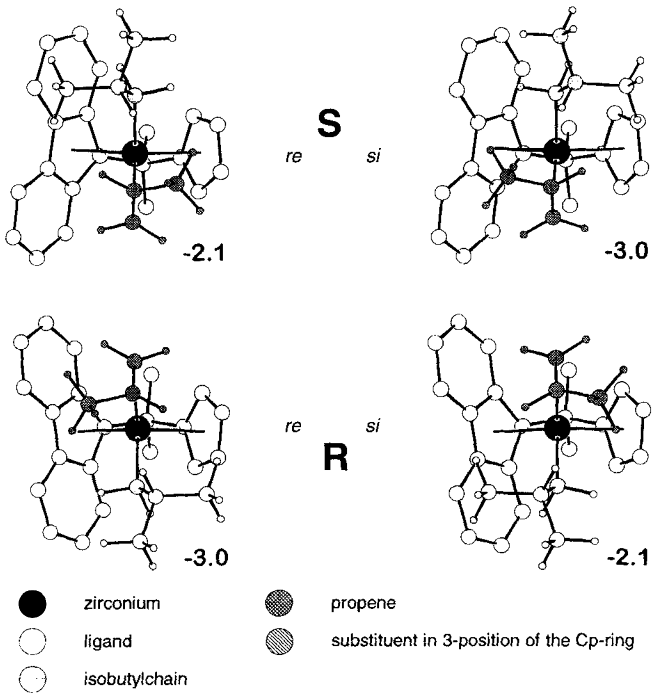

Figure 2. Minimum-energy diastereomers of [{*i*Pr(CpFlu)}Zr(propene)(isobutyl)] (energies in kcal mol^{-1}).

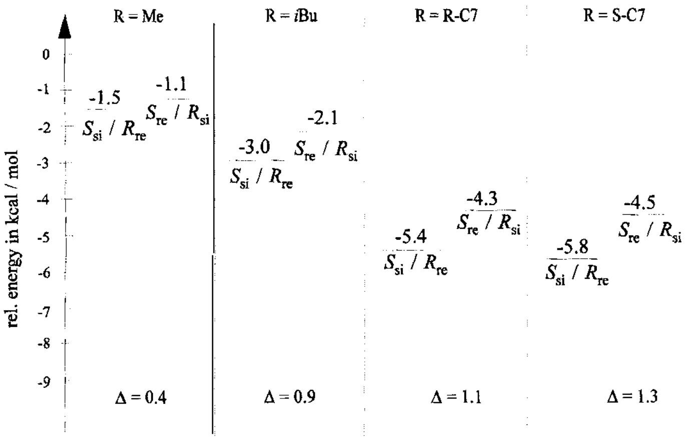

Figure 3. Energy differences between the diastereomers of [{*i*Pr(CpFlu)}Zr(propene)(alkyl)].

The difference in energy between *re* and *si* coordination of the propenes is only 0.4 kcal mol^{-1} for R = Me (1st insertion step), 0.9 kcal mol^{-1} for R = *i*Bu (2nd insertion step), and 1.1 or 1.3 kcal mol^{-1} for R = (*R*)-dimethylpentyl and (*S*)-dimethylpentyl, respectively (abbreviated as R-C7 and S-C7 in Figure 3). Energy differences of at least 1 kcal mol^{-1} are considered to be significant, for which the error is estimated to be ±0.5 kcal mol^{-1}.[13] Therefore, only the second propene insertion step is specific. With (*R*)-configurated Zr, the *re* coordination of propene is preferred in each case; with (*S*)-configurated Zr, *si* coordination is preferred. This trend continues for R = R-C7 and S-C7. With isobutyl as the polymer chain, Figures 2 and 3 indicate that R_{re} and S_{si} are lowest in energy (−3.0 kcal mol^{-1}). Thus, the catalyst changes (during insertion) back and forth between these chiralities ($R_{re} \leftrightarrow S_{si}$). In other words, the catalyst yields a syndiotactic polymer.

[{*i*Pr(3-Me-CpFlu)}Zr(alkyl)(propene)]: The calculation of the intermediate stages of the [{*i*Pr(3-Me-CpFlu)}ZrCl$_2$] catalyst, yielded eight diastereomers (four pairs of enantiomers), because of the additional chirality induced by the 3-Me-Cp ring. Figure 4 depicts the structures of the four energetically different diastereomers with (*R*) configuration at the 3-Me-Cp ring. The energy of the R_{re} conformer is remarkably low. Here, the growing polymer chain possesses the highest degree of freedom. The conformers S_{re}, S_{si}, and R_{si} have similar energies (Figures 4 and 5). The energy difference $\Delta R_{re} - R_{si}$ is 1.8 kcal mol^{-1}; the energy difference $\Delta S_{re} - S_{si}$ is only 0.2 kcal mol^{-1}.

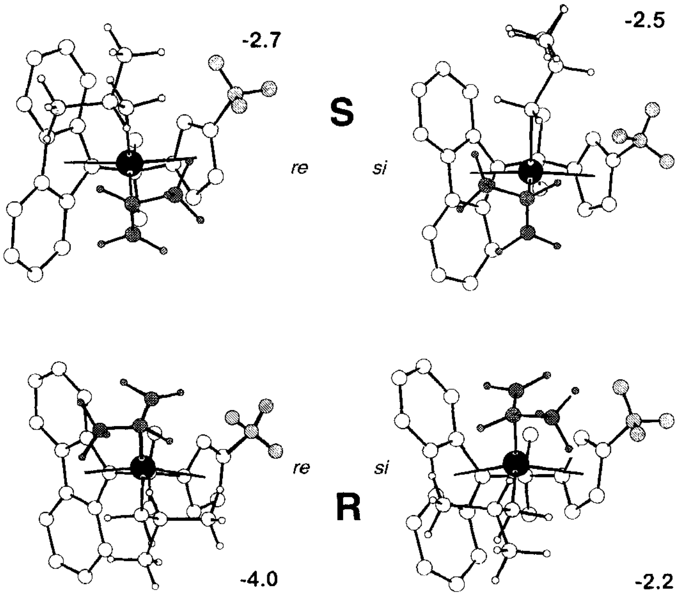

Figure 4. Minimum-energy diastereomers of [{*i*Pr(3-Me-CpFlu)}Zr(propene)(isobutyl)] (energies in kcal mol^{-1}; for explanation of shadings, see Figure 2).

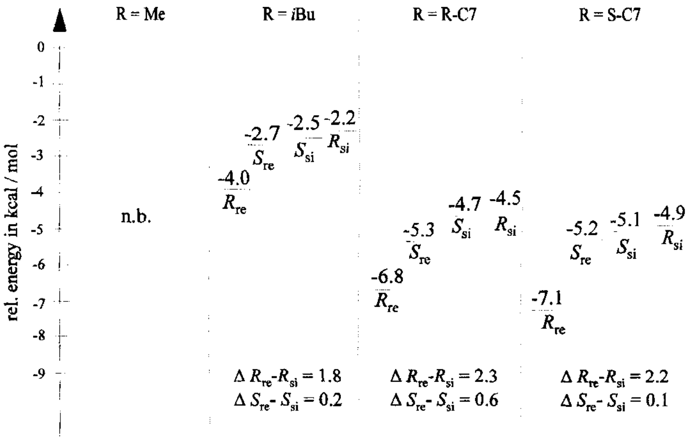

Figure 5. Energy differences between diastereomers of [{*i*Pr(3-Me-CpFlu)}Zr(propene)(alkyl)].

During polymerization, propene preferentially coordinates to (R)-configurated Zr at the *re* face, whereas there is no preference for the *re* or *si* face with (S)-configurated Zr. This means the first, third, fifth etc. methyl groups of the growing polymer chain are isotactic and the second, fourth, sixth etc. are statistically arranged. The resulting polypropylene is thus hemiisotactic.

[{*i*Pr(3-*t*Bu-CpFlu)}Zr(alkyl)(propene)]: Figure 6 shows four of the eight possible diastereomeric structures of [{*i*Pr(3-*t*Bu-CpFlu)}Zr(propene)(isobutyl)], in each case with (R) configuration at the 3-*t*Bu-Cp ring. In this example the R_{re} conformation is also lowest in energy. However, what is remarkable and new is that, after the first insertion step, *re* coordination also occurs preferentially at the (S)-configurated Zr. In addition to the interactions between the ligand and the polymer chain, strong interactions seem to be taking place between the *tert*-butyl substituent at the Cp-ring and the methyl group of the propene. This explains the high energy of the R_{si} conformer.

After the first insertion step, the energy difference $\Delta R_{re} - R_{si}$ is 2.8 kcal mol^{-1}; the energy difference $\Delta S_{re} - S_{si}$ is 1.5 kcal mol^{-1} (Figure 7). The noticeable preference towards *re* coordination of the propene molecule, for both (R)- and (S)-configurated zirconium centers, leads to a sequence of m diads, that is, to the formation of isotactic polypropylene. In other words, in contrast to the previous methyl-substituted catalyst, we now have a differentiation between *re* and *si* faces, that is, R_{re} and S_{re} lie much lower in energy than R_{si} and S_{si}. The catalyst species now changes back and forth between R_{re} and S_{re} (Figure 6) during the course of insertion. In other words, the catalyst now works isotactically. Figure 8 summarizes the relative energies of the four diastereomers of the different catalysts (with an isobutyl group as the polymer chain).

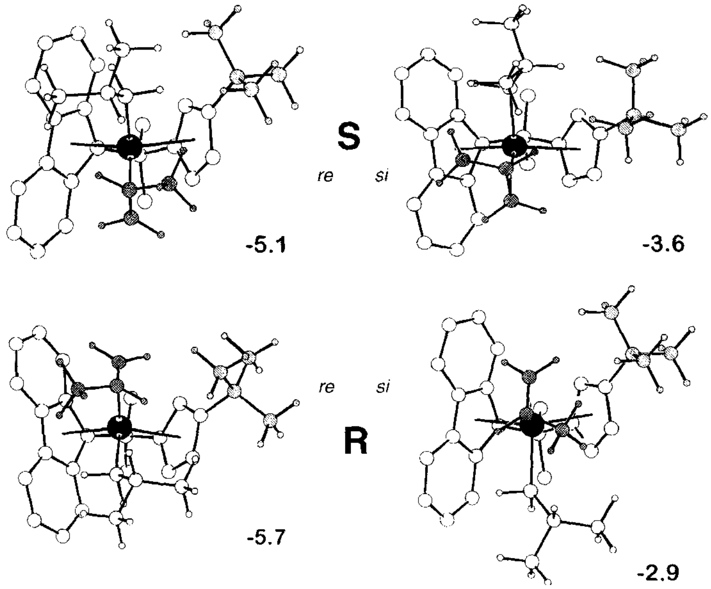

Figure 6. Minimum-energy diastereomers of [{*i*Pr(3-*t*Bu-CpFlu)}Zr(propene)(isobutyl)] (energies in kcal mol^{-1}; for explanation of shadings, see Figure 2).

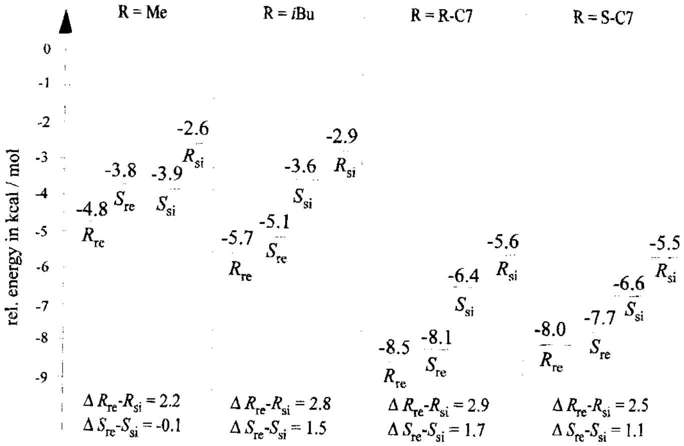

Figure 7. Energy differences between diastereomers of [{*i*Pr(3-*t*Bu-CpFlu)}Zr(propene)(alkyl)].

Now it becomes clear that it is not the symmetry of the catalysts that is decisive for the stereospecificity, but the energy gradations, in particular the size of the energy gap between the individual diastereomeric states. Thus, catalyst I operates syndiotactically because $R_{re} = S_{si} < S_{re} = R_{si}$, catalyst II hemiisotactically because $R_{re} < S_{re}$, S_{si}, R_{si}, catalyst III isotactically because R_{re}, $S_{re} < S_{si}$, R_{si}, and catalyst IV atactically because $R_{re} \approx S_{re}$, S_{si}, R_{si}. The "symmetry rule" still applies, but is not the only decisive factor; it is only one aspect of our universal model.

A good model must enable us to predict results. We therefore synthesized catalyst V ([{*i*Pr(3-*i*Pr-CpFlu)}ZrCl$_2$]), which should fit in between catalysts II and III in Figure 8, based on

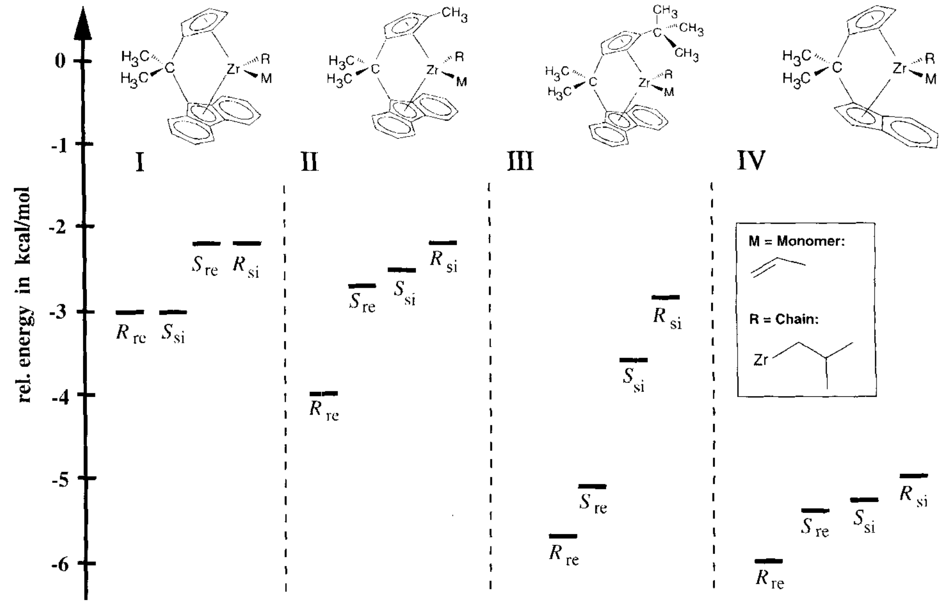

Figure 8. Comparison of the energy differences between the diastereomers for the catalysts I-III and IV (ref. [14]).

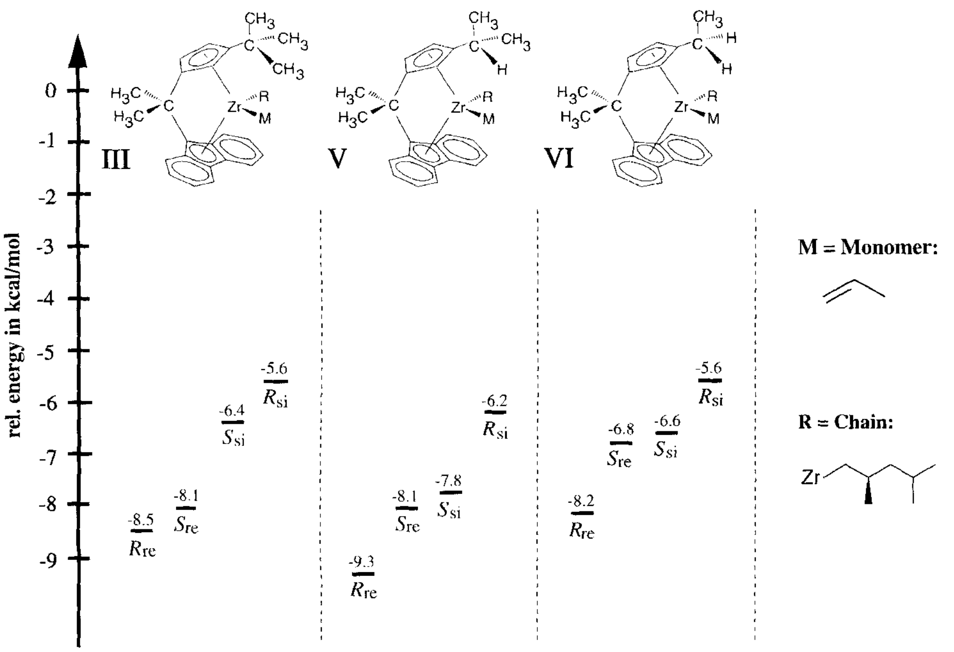

Figure 9. Comparison of the energy differences between the diastereomers for a number of catalysts.

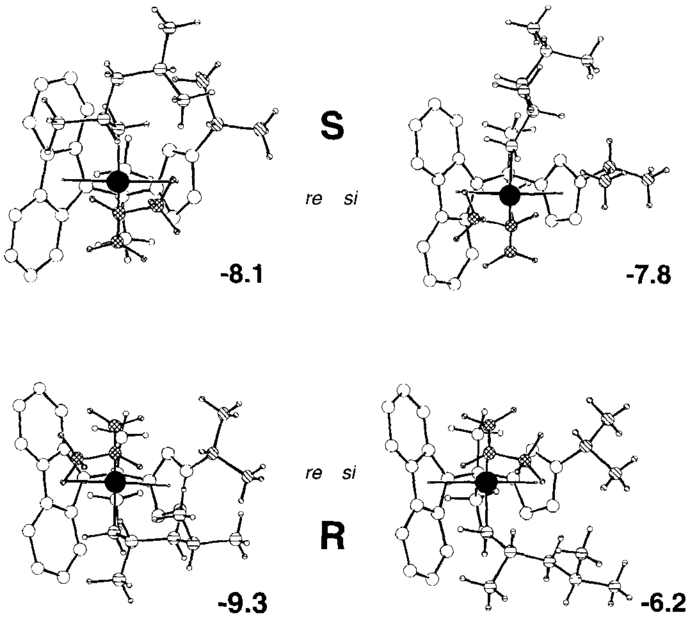

Figure 10. Minimum-energy diastereomers of [{*i*Pr(3-*i*Pr-CpFlu)}Zr(propene)(2,4-dimethylpentyl)] (energies in kcal mol^{-1}; for explanation of shadings, see Figure 2).

its steric requirements. The molecular modeling calculations (Figures 9 and 10) predict that catalyst V should produce hemiisotactic polypropylene, since the decisive energy gap now lies between the conformational states R_{re} and S_{re}, S_{si}. This was confirmed by experiment: catalyst V was indeed found to give hemiisotactic polymer.

Our model has been shown to be capable of predicting the microstructure of a polymer, based on the substitution pattern in the ligand of the catalyst. The syntheses of further catalysts, such as [{*i*Pr(3-Et-CpFlu)}ZrCl$_2$] (VI, Figure 9) and [{*i*Pr(3-*i*Pr-CpInd)}ZrCl$_2$], related to IV (Figure 8), are in progress.

Finally, we turn to the interesting subject of stereoerrors. Even these can be classified and explained through our model. Figure 11 presents ^{13}C NMR spectra (methyl region) of syndiotactic, hemiisotactic, and isotactic polypropylene obtained with [{*i*Pr(CpFlu)}ZrCl$_2$], [{*i*Pr(3-Me-CpFlu)}ZrCl$_2$], and [{*i*Pr(3-*t*Bu-CpFlu)}ZrCl$_2$], respectively, under similar conditions in each case.

The stereospecificity of the metallocenes is temperature dependent. The rrrr pentad of the syndiotactic polypropylenes decreases, for example, from 93% at $T_p = 10\,^{\circ}C$ to 58.6% at $T_p = 70\,^{\circ}C$.[17] With increasing polymerization temperatures, an increase of the pentads mmmm,

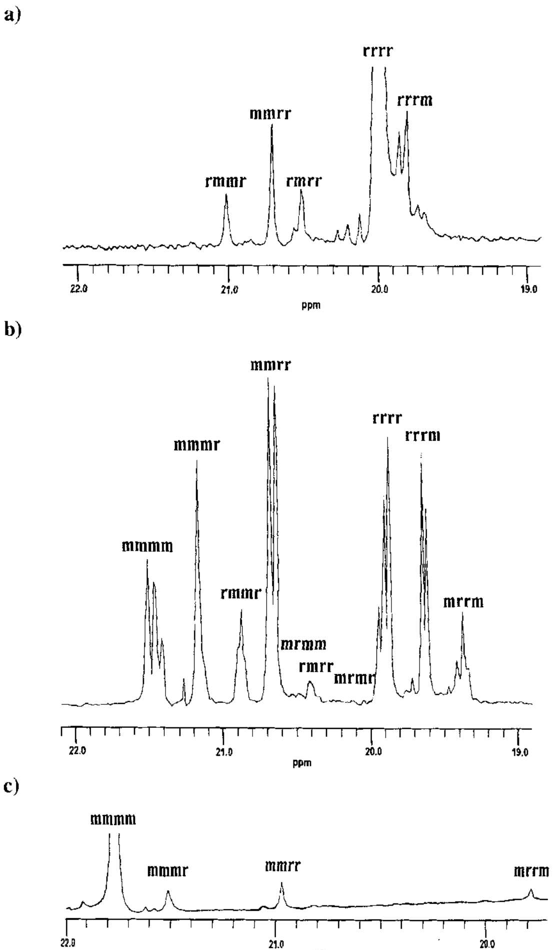

Figure 11. ^{13}C NMR spectra of a) syndiotactic polypropylene, catalyst [{*i*Pr-(CpFlu)}ZrCl$_2$]/MAO, polymerization at $P = 2$ bar, $T_p = 30\,^{\circ}C$, [Zr] = 9.72×10^{-6} mol L^{-1}, [Al]:[Zr] = 1970:1 in toluene; b) hemiisotactic polypropylene, catalyst [{*i*Pr(3-Me-CpFlu)}ZrCl$_2$]/MAO, polymerization at $P = 2$ bar, $T_p = 30\,^{\circ}C$, [Zr] = 3.71×10^{-5} mol L^{-1}, [Al]:[Zr] = 1550:1 in toluene; c) isotactic polypropylene, catalyst [{*i*Pr(3-*t*Bu-CpFlu)}ZrCl$_2$]/MAO, polymerization at $P = 2$ bar, $T_p = 35\,^{\circ}C$, [Zr] = 4.65×10^{-5} mol L^{-1}, [Al]:[Zr] = 2094:1 in toluene.

mmmr, and mrrm is obtained in hemiisotactic polypropylene, whereas the pentads rmmr, mmrr, rrrr, and rrmm are reduced. Each of the ten possible pentads can be produced by passing through a sequence of conformers (Figure 12).

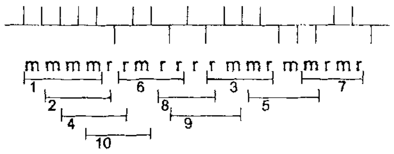

mmmm:	$R_{re} \rightarrow$	$S_{re} \rightarrow$	$R_{re} \rightarrow$	$S_{re} \rightarrow$	R_{re}
mmmr:	$R_{re} \rightarrow$	$S_{re} \rightarrow$	$R_{re} \rightarrow$	$S_{re} \rightarrow$	R_{si}
rmmr:	$R_{re} \rightarrow$	$S_{si} \rightarrow$	$R_{si} \rightarrow$	$S_{si} \rightarrow$	R_{re}
mmrr:	$R_{re} \rightarrow$	$S_{re} \rightarrow$	$R_{re} \rightarrow$	$S_{si} \rightarrow$	R_{re}
mrmm:	$R_{re} \rightarrow$	$S_{re} \rightarrow$	$R_{si} \rightarrow$	$S_{si} \rightarrow$	R_{si}
rmrr:	$R_{re} \rightarrow$	$S_{si} \rightarrow$	$R_{si} \rightarrow$	$S_{re} \rightarrow$	R_{si}
mrmr:	$R_{re} \rightarrow$	$S_{re} \rightarrow$	$R_{si} \rightarrow$	$S_{si} \rightarrow$	R_{re}
rrrr:	$R_{re} \rightarrow$	$S_{si} \rightarrow$	$R_{re} \rightarrow$	$S_{si} \rightarrow$	R_{re}
rrrm:	$R_{re} \rightarrow$	$S_{si} \rightarrow$	$R_{re} \rightarrow$	$S_{si} \rightarrow$	R_{si}
mrrm:	$R_{re} \rightarrow$	$S_{re} \rightarrow$	$R_{si} \rightarrow$	$S_{re} \rightarrow$	R_{re}

Figure 12. Top: ten possible pentads of polypropylene [14,18]. Bottom: sequence of configurations that are passed through to generate the pentads.

Basically, any pentad is allowed for any catalyst. The frequency of a pentad is determined by the probability that a specific conformer is adopted during an insertion step; this probability in turn depends on the energy content of the intermediate states or the size of the energy gap between *re* and *si* conformers for (*R*)- and (*S*)-configurated zirconium centers. In other words, by means of the pentad distribution obtained experimentally, it is possible to deduce which conformers have been passed through. In syndiotactic polypropylenes, m diads and mm triads appeared especially frequently as errors. Through stereoerrors in isotactic polypropylene, rr triads are produced. In the case of hemiisotactic polypropylenes, the mrmm, rmrr, and mrmr pentads are forbidden. The mrmm and rmrr pentads only show up at increased polymerization temperatures. The pentad mrmr fails to appear altogether.[17, 19]

The occurrence of the mrmm and rmrr pentads was explained earlier (see Herfert and Fink[19] as well as Farina[20, 21]) through isomerizations of the growing polymer chain without insertion of a propene molecule. The model described in this publication does not necessarily require intermediate isomerization to explain the formation of the forbidden pentads. When the pentads mrmm, rmrr, and mrmr are compared (Figure 13), it becomes obvious that, in the case of the pentads mrmm and rmrr, only the C atoms C1 and C3 have been arranged in the wrong way relative to each other. In the case of the pentad mrmr, the C atoms C1 and C3 as well as C3 and C5 have been wrongly arranged relative to each other. The probability of a sequential double error is therefore considerably lower.

The model presented above requires no intermediate isomerizations without insertion to explain some of the observed pentads, but does not rule out these isomerizations. Regarding the syndiotactically operating catalyst [{*i*Pr(CpFlu)}ZrCl$_2$], there are two possibilities to explain the pentad rmrr. In the case without intermediate isomerization, after the m-diad the catalyst changes between the two R_{si}/S_{re} conformers, even though these are of higher energy. In the second case, after the m diad an intermediate isomerization without insertion of a propene molecule takes place. The catalyst then changes between the conformers S_{si}/R_{re}, which are of lower energy.

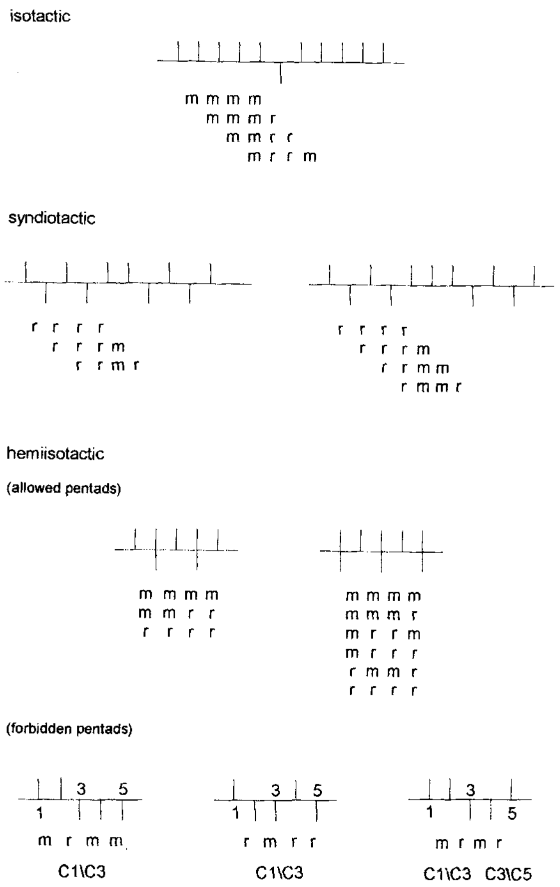

Figure 13. Pentad errors occurring in isotactic, syndiotactic, and hemiisotactic polypropylene.

Conclusion

By means of the pentad distribution obtained by experiment, it is possible to reconstruct, with help of the model described above, the identity and sequence of the conformers formed during the growth of a polymer chain. The model can also be used to predict the stereosequence of a polymer chain based on the energy gaps between the different conformers. In this paper we have shown that this energy gap already changes when the substituents at the ligand are modified. At the moment, we are extending the model calculation to encompass a wider variety of bridged metallocene catalysts. Furthermore, we are investigating the following questions:

1) How does the increasing length of the polymer chain affect the reaction?
2) What is the influence of a more sterically demanding monomer (e.g. an α-olefin with a longer side chain)?

3) How do different monomers influence the energy levels of the conformers formed in the course of copolymerization?

Finally, it would be of particular interest to calculate the probability for the formation of a given sequence of conformers as a function of temperature and to attempt a quantitative prediction of the stereoerrors as a function of temperature.

Appendix

Molecular modeling calculations were performed on the catalysts [{*i*Pr(CpFlu)}$ZrCl_2$], [{*i*Pr(3-Me-CpFlu)}$ZrCl_2$, [{*i*Pr(3-*i*Pr-CpFlu)}$ZrCl_2$], and [{*i*Pr(3-*t*Bu-CpFlu)}$ZrCl_2$]. According to Corradini[10, 11, 12] each calculated complex contains a π-coordinated propene molecule, a σ-coordinated alkyl group (R = methyl, isobutyl, (*R*)-2,4-dimethylpentyl, (*S*)-2,4-dimethylpentyl), representing the growing polymer chain, and a bis-η^5-chelating ligand. In valence force-field terms Zr–η^5-Cp bonds and Zr–π bonds cannot usually be calculated. A universal bonding model therefore had to be developed. In this publication we will only apply a qualitative description of basic elements. A detailed explanation is given in ref. [16].

Zr–η^5-Cp bond: Each cyclopentadienyl carbon atom is bonded to a centroid atom in the Cp ring center (Mp, Figure 14). The metal–Cp interaction occurs between the Mp and the formally tetravalent zirconium atom (Zr.t). The centroid atom Mp has the properties of a pseudo-atom (e.g. atom radius 0 Å) and, for reasons of molecular dynamics, the average mass of the ring atoms.

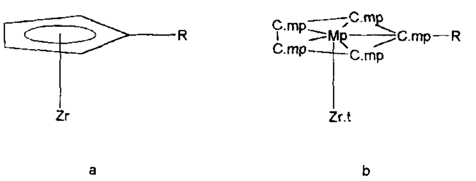

Figure 14. The "centroid" model for the η^5-Cp–Zr bond: a) schematic drawings of the "bonds" used in b; b) labels used for the Zr–Cp π bond.

Zr–η^2 bond: The centroid model can easily be transferred to other types of π bonds like the π bonding between a zirconium atom and a coordinated propene molecule (Figure 15). A pseudo three-membered ring system is used

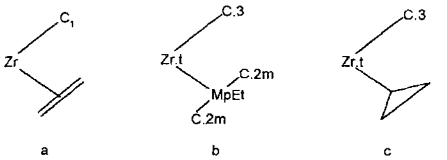

Figure 15. The "centroid" model for the η^2-alkene–Zr bond: a) typical description of the η^2-coordination; b) labels in the Zr–alkene π bond; c) schematic representation of the "bonds" used in b.

with the centroid MpEt located in the middle of the alkene double bond. A σ bond connects the zirconium atom and MpEt. Calculations by M. Nolte[13, 16] show that the alkene π bonds of energy-minimized structures are located in the plane formed by MpEt, Zr, and C_1 (Figure 16). Owing to the defined torsion twisting potential, which describes the rotation around the Zr–MpEt bond, the coordinated propene molecule is forced to remain in plane, with only small deviations (about 10° [13]) being allowed. The force-field calculations are based on crystal structure data of the catalyst [{*i*Pr(CpFlu)}$ZrCl_2$]. By replacing both chlorine atoms with a σ-coordinated alkyl group and a π-coordinated propene molecule, respectively, the energies of all possible diastereomers were calculated. For the bonds that are able to rotate freely (Figure 17), a number of energetically favorable conformations were found. The lowest-energy conformation were determined by optimizing the molecule structure.

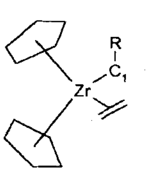

Figure 16. Arrangement of the Zr–alkene π bond in the plane formed by MpEt, Zr, and C_1.

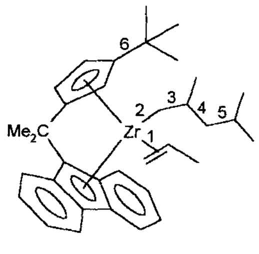

Figure 17. [{*i*Pr(3-*t*Bu-CpFlu)}Zr(propene)-(2,4-dimethylpentyl)]. Free rotation (360°) is possible about bonds 1–5 and 120° rotation about bond 6.

Acknowledgement: We would like to thank J. Kuhnigk, who works in the X-ray Department of our institute, for supplying the Figures.

Received: September 23, 1996 [F474]

[1] W. Kaminsky, K. Külper, H. H. Brintzinger, F. R. W. P. Wild, *Angew. Chem.* **1985**, *97*, 507; *Angew. Chem. Int. Ed. Engl.* **1985**, *24*, 507

[2] J. A. Ewen, R. L. Jones, A. Razavi, *J. Am. Chem. Soc.* **1988**, *110*, 6255.

[3] W. Spaleck, M. Antberg, M. Aulbach, B. Bachmann, V. Dolle, S. Hafka, F. Küber, J. Rohrmann, A. Winter (*New Isotactic Polypropylenes via Metallocene Catalysts*) in *Ziegler Catalysts, Recent Scientific Innovations and Technological Improvements* (Eds.: G. Fink, R. Mülhaupt, H. H. Brintzinger), Springer, Berlin, **1995**, 83.

[4] W. Spaleck, F. Küber, A. Winter, J. Rohrmann, B. Bachmann, M. Antberg, V. Dolle, E. F. Paulus, *Organometallics* **1994**, *13*, 954.

[5] M. Aulbach, F. Küber, *Chem. Unserer Zeit* **1994**, *28*, 197.

[6] U. Stehling, J. Diebold, R. Kirsten, W. Röll, H. H. Brintzinger, S. Jüngling, R. Mülhaupt, F. Langhauser, *Organometallics* **1994**, *13*, 964.

[7] F. Langhauser, J. Kerth, M. Kersting, P. Kölle, D. Lilge, P. Müller, *Angew. Makromol. Chem.* **1994**, *223*, 155.

[8] J. A. Ewen, M. J. Elder, European Patent Application 537130, 1992.

[9] M. Reffke, diploma thesis, Heinrich-Heine-Universität Düsseldorf, **1995**.

[10] P. Corradini, G. Guerra, *Prog. Polym. Sci.* **1991**, *16*, 239.

[11] L. Cavallo, G. Guerra, M. Vacatello, P. Corradini, *Macromolecules* **1991**, *24*, 1784.

[12] a) P. Corradini, V. Busico, R. Cipullo, *Makromol. Chem. Rapid Commun.* **1992**, *13*, 21. b) G. Guerra, P. Corradini, L. Cavallo, M. Vacatello, *Makromol. Symp.* **1995**, 307

[13] M. Nolte, dissertation, Westfälische Wilhelms-Universität Münster, **1992**.

[14] P. Montag, Y. v. d. Leek, K. Angermund, G. Fink, *J. Organomet. Chem.* **1995**, *497*, 201.

[15] TRIPOS Assoc., St. Louis, USA, Version 6. X.

[16] K. Angermund, A. Hanuschik, M. Nolte (*Forcefield Calculations on Zirconocene Compounds*) in *Ziegler Catalysts, Recent Scientific Innovations and Technological Improvements* (Eds.: G. Fink, R. Mülhaupt, H. H. Brintzinger), Springer, Berlin, **1995**, 251.

[17] G. Fink, N. Herfert, P. Montag (*The Relationship between Kinetics and Mechanisms*) in *Ziegler Catalysts, Recent Scientific Innovations and Technological Improvements* (Eds.: G. Fink, R. Mülhaupt, H. H. Brintzinger), Springer, Berlin, **1995**, 159.

[18] P. Montag, dissertation, Heinrich-Heine-Universität, Düsseldorf, **1995**.

[19] N. Herfert, G. Fink, *Makromol. Chem. Macromol. Symp.* **1993**, *66*, 157.

[20] M. Farina, G. Di Silvestro, P. Sozzani, *Macromolecules* **1993**, *26*, 946.

[21] M. Farina, G. Di Silvestro, A. Terragni, *Macromol. Chem. Phys.* **1995**, *196*, 353.

0947-6539/97/0304-0591 $ 17.50+.50/0